INL/CON-21-63469-Revision-0

Persistent Acoustic Sensing for Monitoring A Reactor Facility

July 2021

Edna S Cardenas, John F. Krebs, Scott M Watson, James T Johnson, Jay D Hix, David L Chichester, Milton A. Garces

Changing the World's Energy Future

INL is a U.S. Department of Energy National Laboratory operated by Battelle Energy Alliance, LLC

INL/CON-21-63469-Revision-0

Persistent Acoustic Sensing for Monitoring A Reactor Facility

Edna S Cardenas, John F. Krebs, Scott M Watson, James T Johnson, Jay D Hix, David L Chichester, Milton A. Garces

July 2021

Idaho National Laboratory
Idaho Falls, Idaho 83415

http://www.inl.gov

Prepared for the
U.S. Department of Energy
Under DOE Idaho Operations Office
Contract DE-AC07-05ID14517

Persistent Acoustic Sensing for Monitoring A Reactor Facility

E. S. Cárdenas[1], M. A. Garcés[2], J. F. Krebs[3], S. M. Watson[1], J. T. Johnson[1], J. D. Hix[1], and D. L. Chichester[1]

1. Idaho National Laboratory, Idaho Falls, Idaho
2. University of Hawai'i, Manoa, Hawai'i
3. Argonne National Laboratory, Lemont, Illinois

ABSTRACT

Measurements over the past few years, taking place within the Multi-Informatics for Nuclear Operations Scenarios project, show that infrasound and low-frequency acoustic monitoring can detect, and often quantify, activities that occur on-site at the High Flux Isotope Reactor. Observable activities include: crane translation, lifting, and lowering; differentiation between loaded and unloaded crane operations; access door opening and closing; vehicle operations; and cooling tower fan operations. Advanced data analytic and spectral feature extraction methods can be used to interpret selected signatures to reach a deeper understanding of different reactor activities. These measurements are being conducted using a network of smartphones that continuously operate in conjunction with cloud-based architectures. A recent addition to the system is the development and deployment of a real-time, cloud-based analytic framework that supports near-real-time alarming which can facilitate tip-and-cue protocols. This paper presents recent research in this area including the use of low-frequency acoustics to tip-off transfer operations and cue a more comprehensive analysis by other sensor networks.

INTRODUCTION

The Multi-Informatics for Nuclear Operations Scenarios (MINOS) project is a multi-laboratory collaboration established to characterize persistent monitoring data collected in and around the High Flux Isotope Reactor (HFIR) and the Radiochemical Engineering Development Center (REDC) located at Oak Ridge National Laboratory (ORNL) [1,2]. The general focus of MINOS is to fuse data collected from multiple sensing modalities and characterize operations occurring at nuclear facilities. HFIR provides a high flux of neutrons that are used to conduct experiments by researchers in various fields. Located in REDC are equipment and instrumentation used for the chemical processing of radioisotopes. In both facilities nuclear materials are produced and transferred, therefore they provide a suitable testbed for monitoring operations.

In the MINOS venture, sensing devices measure electromagnetic, radiation, thermal, seismic, infrasound and low-frequency acoustics from nuclear operations. Currently, the infrasound and low-frequency acoustic sensing devices use the RedVox Infrasound Recorder mobile application and the built-in microphone on Samsung Galaxy S10 smartphones. At the present time there are 10 smartphones collecting data at the ORNL testbed. Data are streamed from the RedVox application to the Amazon cloud then continue to a data pipeline at Lawrence Livermore National Laboratory where they are ultimately transferred to a web portal at Lawrence Berkeley National Laboratory.

Over the last few years MINOS researchers have been able to identify nuclear reactor operations such as cooling tower fan speeds, vehicle movements in transfer events, reactor operational states, and

specific aspects of dissolution events [3-8]. Although interest continues in the characterization of these events, this work focuses on nuclear transfer operations. To further this research some of the smartphone sensing devices installed at ORNL are positioned strategically between HFIR and REDC to record transfer operations between the two facilities. Specific operations of interest include the transfer of spent fuel, Sugarman casks, and the Q-Ball radioactive material shipping cask. Typically, heavier material transfers include the movement of materials on a vehicle that may include a flatbed truck, a trailer and a flatbed truck, or a vehicle with up to 5 axles. The vehicle will drive up to a facility, the airlock door will open at the facility, the vehicle will drive in, and then the door will close. After the material is loaded onto the vehicle the airlock door will open to allow the vehicle to exit, then the door will close, and finally the shipment will be transferred. A more reliable picture of the operation of interest can be achieved by fusing data collected from disparate local sensors in contrast to relying on a single sensing modality. For example, in the case of a materials transfer, acoustic and/or seismic sensors may be able to determine the presence of a heavy truck, acoustics and/or electromagnetic sensors may detect the movement of a garage/airlock door, and radiation sensors may detect the presence of radioactive materials and the path of the transfer event. In this example, one sensor type may verify the operation initially determined by an alternate sensor type.

This research is focused on the development of low-frequency acoustic signatures and a programmed algorithm that informs transfer operations. Transfers may be identified by acoustic signals generated from opening and closing the exterior HFIR truck airlock door. The notification of operations will provide time frames in which to focus further data analysis efforts. This work is intended to facilitate follow-up investigation using data collected by disparate local sensors and a more in-depth acoustic analysis as well as the potential implementation of near-real-time analysis on cloud-based platforms.

EQUIPMENT AND METHODS

During the week beginning November 11, 2019, the infrasound and low-frequency acoustic team recorded unplanned and directed operations at the ORNL testbed. In addition, the team video recorded operations time-synched to the acoustic sensing smartphones via a connection to the Global Positioning System. Directed operations were recorded of the exterior truck airlock door at HFIR for signature discovery. A video capture of the tilt-up style airlock door with a view of a truck inside the airlock is shown in Figure 1(a). On November 13, 2019, the team, with help from ORNL staff, arranged to have the exterior truck airlock door opened and closed three times. The recorded times and duration of these activities are listed in columns 2-4 in Table 1.

The acoustic sensing smartphone, identification number 35, in nearest proximity to the exterior HFIR truck airlock door is located on the outside of the airlock and around the corner from the door, as shown in Figure 1(b). Due to its proximity, smartphone 35 is best suited for the recording and discovery of acoustic signals generated from the HFIR truck airlock; therefore, all graphs displayed in this paper are generated from smartphone 35 data. Smartphone 35 is installed in a weatherized enclosure, mounted 1 m from the ground, and set at an acoustic sampling rate of 800 Hz. The time and frequency bin widths are approximately 5 s and 0.1 Hz, respectively, for all spectrograms shown in this paper. A spectrogram created during the time when the directed airlock door activities took place, is shown in Figure 2. The spectrogram shows a series of power increases at approximately 340 and 360 Hz.

(a) (b)

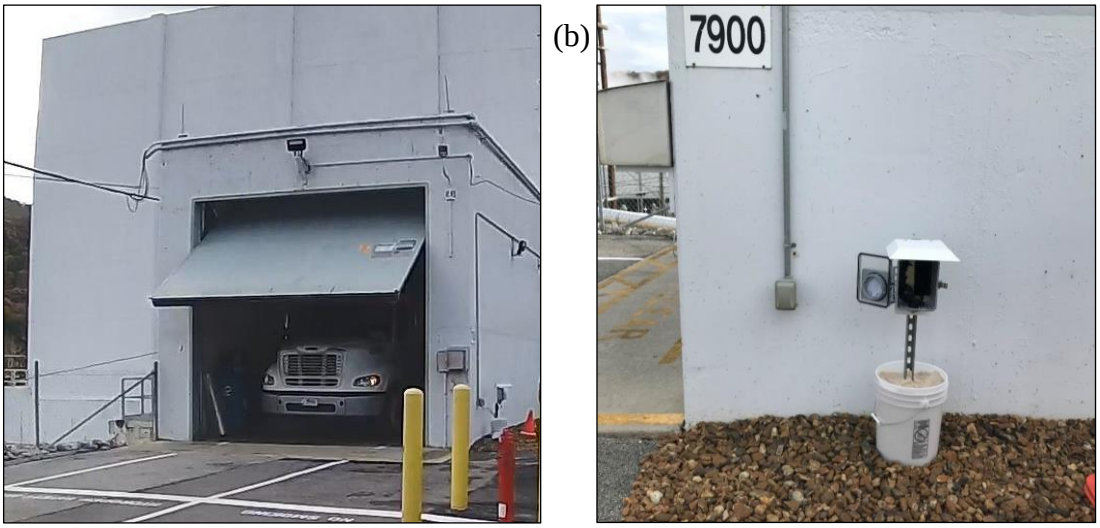

+

Figure 1 Video capture (a) of a truck within the HFIR truck airlock shown behind a tilt-up style door. Acoustic sensing smartphone 35 (b) located around the corner from the exterior HFIR airlock door.

Table 1 Timing and operation information corresponding to the exterior HFIR truck airlock.

Airlock Operation	Recorded Start Time (UTC)	Recorded Finish Time (UTC)	Recorded Duration (s)	Notification Start Time (UTC)	Notification Finish Time (UTC)	Notification Duration (s)
Exterior door opens	18:57:01	18:57:27	26	18:57:01	18:57:21	20
Exterior door closes	18:57:31	18:57:56	25	18:57:21	18:57:42	20
Exterior door opens	18:58:04	18:58:29	25	18:58:06	18:58:27	20
Exterior door closes	18:58:33	18:58:59	26	18:58:26	18:58:47	20
Exterior door opens	18:59:06	18:59:32	26	18:59:10	18:59:30	20
Exterior door closes	18:59:37	19:00:01	24	18:59:30	18:59:51	20

To determine the peak frequency and corresponding edge frequencies of the power increases shown in the spectrogram, power spectra were created for each time frame when the door was opened and closed. The resulting power spectra are shown in Figure 3. Figure 3(a) and Figure 3(b) show power curves when the airlock door was opened and closed, respectively. Both spectra a show peak, at approximately 360 Hz, generated when the airlock door was opened and closed. In addition, the power spectra show that when the airlock door is opened a smaller peak is generated at approximately 380 Hz while a peak at approximately 340 Hz is generated when the airlock door is closed. The 360-Hz peak amplitude and edges, determined from the power spectra, were used to program a signal notification algorithm.

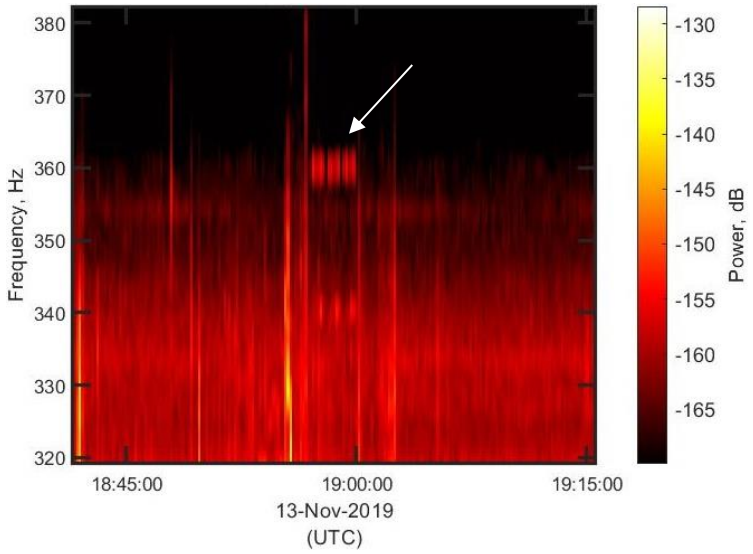

Figure 2 Spectrogram generated with data collected during known times when the HFIR exterior airlock door opened and closed on November 13, 2019. The white arrow points to a series of power increases with the initial increase beginning at approximately 18:56:59 UTC and the final increase ending at approximately 18:59:58 UTC. Times were determined from the spectrogram.

The signal notification algorithm was written in MATLAB® and incorporates a two-sample t-test function that returns a decision on the equality between the distribution of two input samples. The input samples include frequency ranges that envelope 1) the 360-Hz peak and 2) background frequencies. For both samples, the frequency ranges were determined from the power spectra detailed in Figure 3. The 360-Hz peak has -11 to -15 dB points at 355.5 Hz and 364.6 Hz, respectively. The background noise incorporates frequencies slightly lower and slightly higher than the 360-Hz peak; the lower background frequencies range from 351.3 to 355.3 Hz and the higher frequencies range from 364.8 and 368.8 Hz. The background sample merges both background frequency ranges. To enhance the signal-to-noise, the power in these frequency ranges were squared before input into the t-test function. The difference between normalized squared and unsquared power values and background power is displayed in Figure 4. The samples in the graph result from data collected during the first directed opening and closing of the airlock door on November 13, 2019. The channels extend from channel 326 (18:57:01 UTC) to channel 333 (18:57:42 UTC). The power in the graph is normalized to the smallest power in the background sample and shows that the ratio of the mean power between the background and the 360-Hz peak increases by a minimum of 2 times and a maximum of 30 times when the samples are squared. In addition, the t-test function includes options that specify that the mean of the 360-Hz peak must be larger than the mean of the background to a significance level of 5%. Furthermore, for a signal to notify, the power increase must persist for between 19 and 27 s to include the length of time it takes to open or close the airlock door. This length of time was determined from the recorded duration listed in Table 1 and from the video recorded during the directed airlock door activities. Due to the time length and the approximate 5 s time bins, the notification time length remains at 20 s for all events identified in this research.

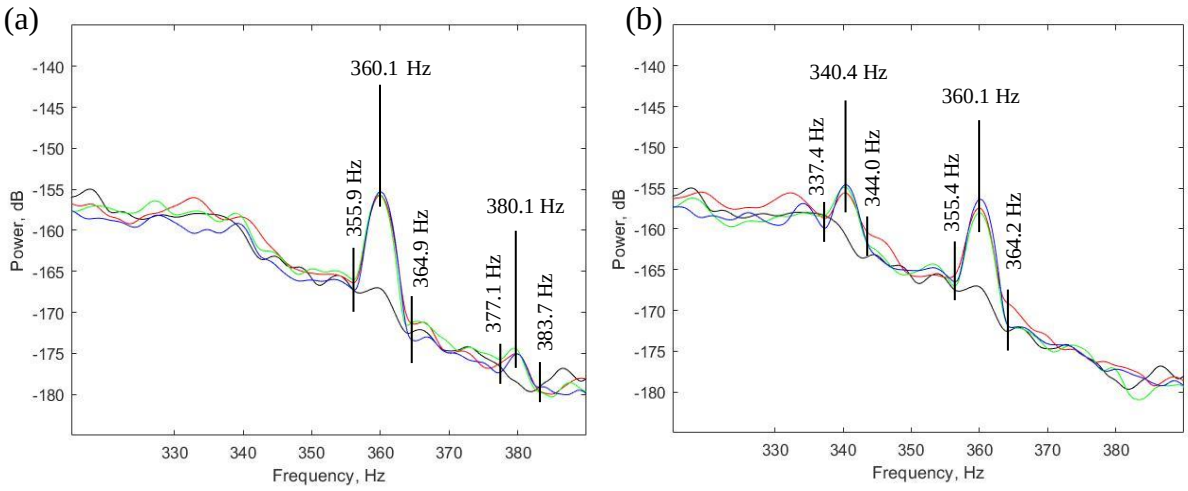

Figure 3 Power spectra showing peaks generated when the HFIR airlock door was opened (a) and closed (b). The background (—) includes data that starts 15 s before the initial airlock door operation and continues for 10 s. Signal curves include 20 s of data from the start of each airlock door operation.

For transfer events it is likely that two signals will occur; one shortly after the other. A repeated signal would signify that the airlock door opened, a truck either entered or exited the airlock, and finally the airlock door closed. This signature of a repeated signals has not been implemented into the algorithm, but can be used for verification of airlock door operations.

ANALYSIS AND RESULTS

The notification algorithm was initially implemented on the directed airlock door activities on November 13, 2019. The results of the algorithm are listed in the last three columns in Table 1. The time differences between the recorded time and the discovered time range between 0 and 14 s. Modifications to the algorithm related to time lengths and bin widths may be required to minimize inconsistencies in the discovered times. Additional testing of the notification algorithm was performed on dates when either there were known times when the airlock door was opened/closed or when there were known potential times when the door was opened/closed.

An example of known HFIR truck airlock door activities occurred on November 12, 2019 when the acoustic team observed the exterior airlock opening, a truck exiting the airlock, and the exterior airlock door closing. These events occurred one after another to facilitate shipment of a used HFIR reactor core to the Savannah River Site. Table 2, columns 2-4, list recorded times observed by the team. The algorithm was implemented on data recorded from approximately 17:00 to 19:30 UTC. The algorithm found three instances where power was increased at approximately 360 Hz, as listed in the last three columns of Table 2. Spectrograms that include the time frame when the HFIR airlock door was known to have opened and closed are displayed in Figure 5. Figure 5(a) shows two notification signals that were not observed by the team and Figure 5(b) shows a notification signal that falls within the time range when the team observed the airlock door closing. In addition, a power increase at 340 Hz is visible in Figure 5(a) and was verified in a power spectrum. This would indicate that the exterior HFIR truck airlock door closed during the notified time from 17:46:02 to 17:46:21

UTC, however, a 380 Hz power increase was not observed between 17:42:33 and 17:42:54 UTC. Although a 380-Hz peak was not generated, the notification signals do occur in succession within a short period of time suggesting the opening and closing of the airlock door. Verification is necessary through analysis from other sensing modalities. Figure 5(b) shows two power increases at 360 Hz, however, the first power increase was not found by the notification algorithm. The algorithm failed at finding the first power increase due to noise at the lower edge of the 360-Hz peak. The succession in short time that occurs by these signals may be an indicator of the opening and closing of the HFIR airlock door.

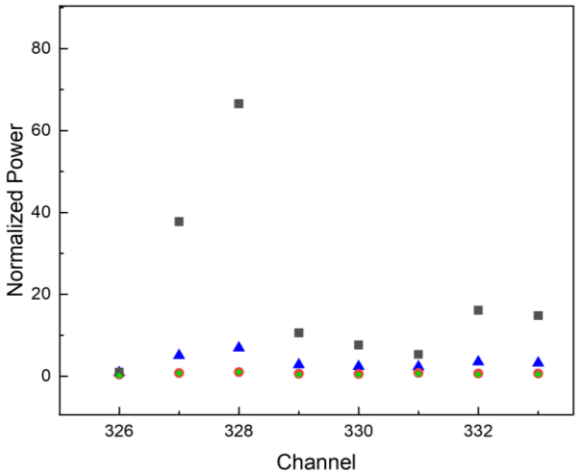

Figure 4 Normalized squared notification signal (■), squared background (♦), unsquared notification signal (▲), and unsquared background (●) power as a function of channel.

Dates of known potential times when the HFIR truck airlock door operated were provided by the MINOS team. An example of a known potential operation was the preparation of spent fuel for shipment on January 27, 2020. The algorithm was implemented and found three notification signals in the hour between approximately 11:00 to 12:00 UTC, as displayed in Figure 6(a). Notification signals were discovered at 11:00:31, 11:04:00, and 11:04:20 UTC. Spectra show an increase in power at approximately 340 Hz for the first and third time frames indicating a door closure. Furthermore, while the second notification signal does not show a power increase at 380 Hz, the second and third notification signals occur in succession over a short time indicating the pattern of an opened and then closed exterior airlock door. The algorithm also discovered 26 notification signals in succession during the hour beginning at approximately 21:30, as displayed in Figure 6(b). These false positive notifications do not match the pattern of the two power increases occurring in short succession and likely were not generated from the HFIR truck airlock door opening and closing. In addition, the 26 notification signals do not show power increases at 340 or 380 Hz. If signals such as these were to be found in near-real-time, additional analysis from acoustic or other local sensors would be required to validate the false positive notifications.

Table 2 Times recorded when a truck exited the HFIR airlock on November 12, 2019.

Airlock Operation	Recorded Start Time (UTC)	Recorded Finish Time (UTC)	Recorded Duration (s)	Notification Start Time (UTC)	Notification Finish Time (UTC)	Notification Duration (s)
Exterior door opens	18:52:34	18:53:00	26	No notification	No notification	
Exterior door closes	18:53:23	18:53:48	25	18:53:26	18:53:46	20
360-Hz peak found	Not observed	Not observed		17:42:33	17:42:54	20
360-Hz peak found	Not observed	Not observed		17:46:02	17:46:21	20

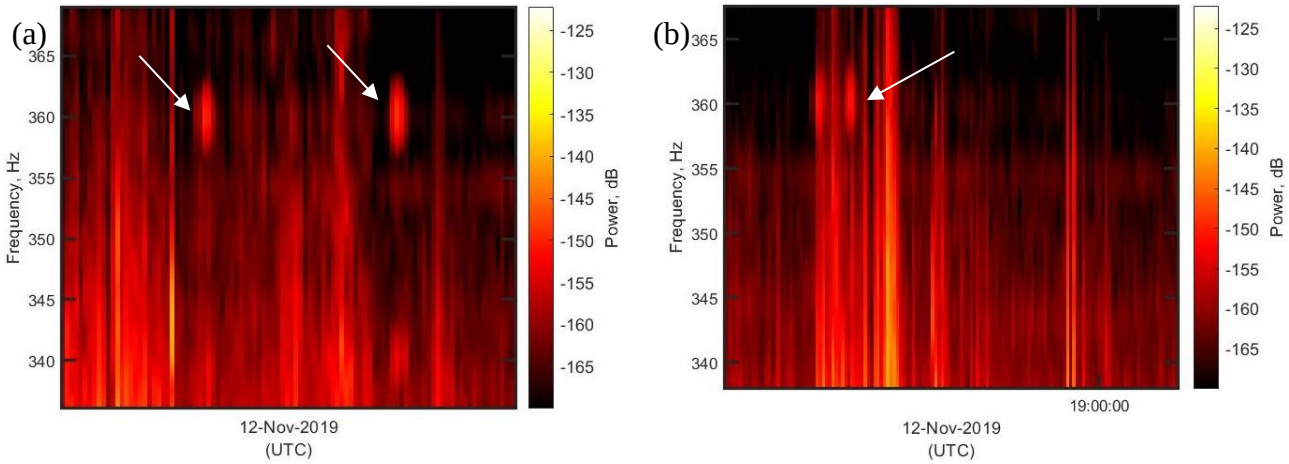

Figure 5 Spectrograms that include known times when the exterior HFIR truck airlock door opened and closed on November 12, 2019. The white arrows point to notification signals.

An additional example of potential known airlock door activities occurred on January 14, 2020 when a Sugarman cask was transferred from the HFIR facility and detected by radiation sensors between 14:42 and 14:46 UTC. The transfer would have occurred before detection from local radiation sensors; therefore, a spectrogram showing data from 14:00 to 15:00 UTC was examined and is shown in Figure 7. Four signals were discovered by the notification algorithm beginning at 14:22:29, 14:23:03, 14:35:43, and 14:36:03 UTC. Power increases at 340 or 380 Hz were not observed, however, power increases in the first and second signals as a pair, and third and fourth signals as a pair, do occur in succession in a short period of time. This pattern may indicate operation of the airlock door opening and closing.

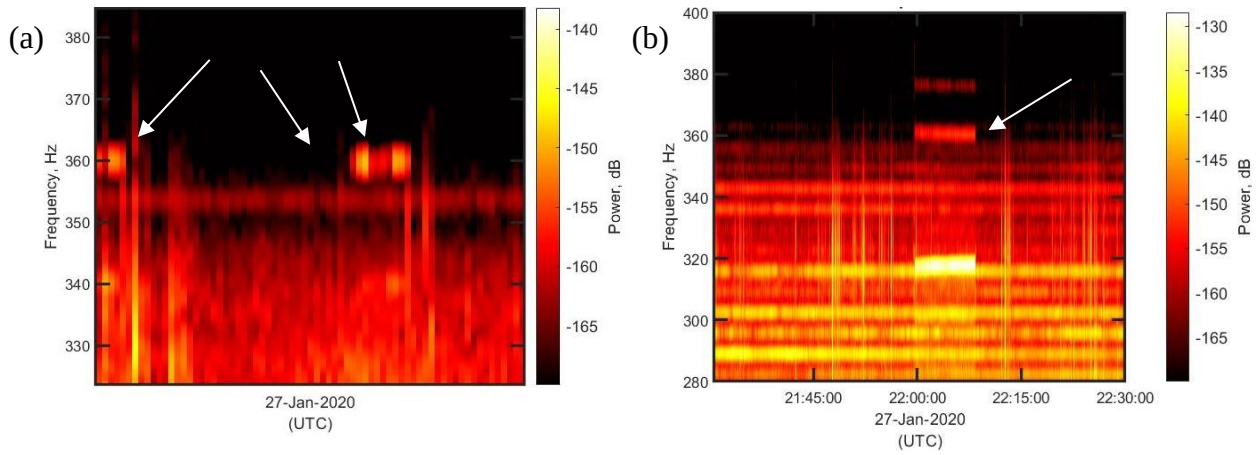

Figure 6 Spectrograms generated from data collected on January 27, 2020 from approximately 11:00 to 12:00 UTC (a) and 21:30 to 22:30 UTC (b). The white arrows point to notification signals.

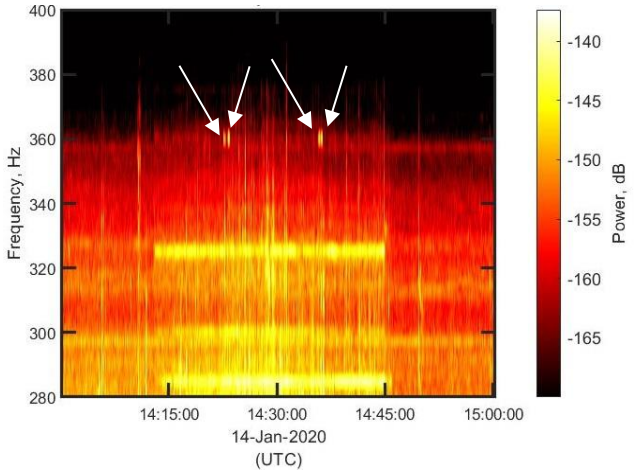

Figure 7 Spectrogram showing notification signals indicated by white arrows.

The notification algorithm was tested on several other dates of potential airlock door activities and successfully discovered signals that match the pattern of signals occurring in succession within several seconds of one another. Validation is required by other local sensors to determine whether the signals were generated from HFIR airlock door activities.

SUMMARY AND FUTURE WORK

Initial work has shown success using a two-sample t-test in conjunction with timing analysis to discriminate signals that are similar in duration and power to those generated when the HFIR truck airlock door opens and closes. The notification algorithm has been implemented on data collected during known times when the airlock door opened and closed and discovered characteristic signals. Furthermore, the algorithm was tested and successfully found characteristic signals from data collected when there was potential for airlock door activity. The algorithm fails when noise is increased around the 360-Hz peak and produces false positive notifications when signals occur within

one-time bin of one another and over many time bins. These limitations can be overcome through further analysis from acoustic or other local sensors and possibly through future modifications of the notification algorithm.

Additional testing on collected data is required to verify the reliability of the programmed notification algorithm. Validation from other local sensors is also necessary to determine if characteristic signals were generated from airlock door activities. Once testing and modifications are complete, additional programming is required to execute the notification algorithm in near-real-time on a cloud-based platform. The discovery of signals at 360 Hz cues further investigation from disparate local sensors aiding in the overall goal of MINOS; to use data from multiple sensing modalities to characterize events occurring at HFIR.

ACKNOWLEDGEMENTS
Work described here was funded by the U.S. National Nuclear Security Administration's Office of Defense Nuclear Nonproliferation Research and Development.

REFERENCES

[1] A. D. Nicholson, D. E. Archer, I. Garishvili, I. R. Stewart and M. J. Willis, "Characterization of gamma-ray background outside of the High Flux Isotope Reactor," *Journal of Radioanalytical and Nuclear Chemistry,* vol. 318, pp. 361-367, 2018.

[2] A. Roy, E. M. Casleton, G. Fairchild and T. A. Nelson, "Feature Detection and Geovisualisation from LiDAR point clouds and Aerial Photography using Bayesian Non Parametric Clustering," in *American Geophysical Union, Fall Meeting*, 2018.

[3] A. E. Egid, E. M. Casleton, D. Chichester, E. Cardenas and M. Garces, "MINOS Infraound Analysis Synopsis," Los Alamos National Laboratory, 2021.

[4] G. Flynn, N. Parikh, D. Archer, T. Karnowski, M. Maceira, O. Marcillo, A. Nicholson, W. Ray, R. Wetherington and M. Willis, "Contraining Data Driven Models for Detection of Sparse, Temporally Correlated Events," in *Next-Gen AI for Proliferation Detection: Domain-Aware Methods Workshop*, 2021.

[5] T. Reichardt, S. Eaton, T. Kulp, S. DeJong, W. Ray, T. Karnowski, R. Wetherington, M. Willis, O. Marcillo, M. Maceira, C. Chengping, E. Cardenas, S. Watson, D. Chichester, C. Gammans, J. Krebs and B. d'Entremont, "Domain-Informed Assessment of Nuclear Reactor Operations," in *Next-Gen AI for Proliferation Detection: Domain Aware Methods Workshop*, Virtual, 2021.

[6] N. Rao, C. Greulich, M. P. Dion, J. Johnson, W. Ray, J. Hite, K. Dayman and R. Hunley, "Dissolution Event Classification Using Isotope Decay Chains and Half-Life Estimates," in *Next-Gen AI for Proliferation Detection: Domain-Aware Methods Workshop*, Virtual.

[7] J. Tibbets, "Node and Region Importance for Classifying Nuclear Operations using Multisensor Arrays," in *Next-Gen AI for Proliferation Detection: Domain-Aware Methods Workshop*, Virtual, 2021.

[8] J. T. Johnson, D. L. Chichester, M. A. Garces, S. M. Watson, A. J. Christie and K. Asmar, "Use of Infrasound to Monitor Nuclear Facilities," in *Institute of Nuclear Materials Management Annual Meeting. 59th 2018*, Baltimore, Maryland, 2018.